REINFORCEMENT DETAILS FOR STRUCTURAL CONCRETE BLAST CONTAINMENT FACILITIES

Krauthammer, T., and Otani, R.K.
Penn State University
University Park, PA 16802

Nickerson, H.
NAVFAC ENG SER CTR-ECDET
Washington, DC 20374

and

Canada, C.
Department of Defense Explosive Safety Board
Alexandria, VA 22331-0600

ABSTRACT

This paper is focussed primarily on the behavior and design of typical three-dimensional slab-to-slab-to-slab joints for monolithic construction of blast containment structures, and the reinforcement details associated with such facilities. The fundamental requirements for all connections were to allow the adjoining members to develop their full structural resistance, to insure adequate performance of the structure, and to avoid unacceptable damage in the connection region. For each case a 3D finite element model of the region of interest was developed, in which different reinforcement configurations were employed. Loading conditions for each case were based on design requirements and data obtained from the literature. These analyses were performed in the nonlinear dynamic domain employing the finite element code DYNA3D. A modified concrete model was introduced, while the steel was represented as individual bars and experimental stress-strain relationships. The observed numerical behavior was used to highlight possible difficulties in current design recommendations, and for evaluating various scenarios that were of interest. The observations, findings and concerns on reinforcement detailing, and a discussion of the corresponding design applications are presented.

INTRODUCTION

Current design procedures for reinforcement details (such as, connections, splices, shear reinforcement, etc.) in structural concrete blast containment facilities are described in TM 5-1300 (1990), however, their actual contribution to resisting applied loads is of interest. This paper describes the numerically simulated anticipated structural response of a specific type of blast containment structure (NCEL, 1990) that was based on TM 5-1300. This study was carried out using the explicit finite element code DYNA3D (1993), as described next.

Report Documentation Page

Form Approved
OMB No. 0704-0188

1. REPORT DATE	2. REPORT TYPE	3. DATES COVERED
AUG 1994		**00-00-1994 to 00-00-1994**

4. TITLE AND SUBTITLE	5a. CONTRACT NUMBER
Reinforcement Details for Structural Concrete Blast Containment Facilities	5b. GRANT NUMBER
	5c. PROGRAM ELEMENT NUMBER
6. AUTHOR(S)	5d. PROJECT NUMBER
	5e. TASK NUMBER
	5f. WORK UNIT NUMBER
7. PERFORMING ORGANIZATION NAME(S) AND ADDRESS(ES) **Naval Facilities Engineering Service Center,ECDET,Washington,DC,20374**	8. PERFORMING ORGANIZATION REPORT NUMBER
9. SPONSORING/MONITORING AGENCY NAME(S) AND ADDRESS(ES)	10. SPONSOR/MONITOR'S ACRONYM(S)
	11. SPONSOR/MONITOR'S REPORT NUMBER(S)

12. DISTRIBUTION/AVAILABILITY STATEMENT
Approved for public release; distribution unlimited

13. SUPPLEMENTARY NOTES
See also ADM000767. Proceedings of the Twenty-Sixth DoD Explosives Safety Seminar Held in Miami, FL on 16-18 August 1994.

14. ABSTRACT
see report

15. SUBJECT TERMS

16. SECURITY CLASSIFICATION OF:			17. LIMITATION OF ABSTRACT	18. NUMBER OF PAGES	19a. NAME OF RESPONSIBLE PERSON
a. REPORT **unclassified**	b. ABSTRACT **unclassified**	c. THIS PAGE **unclassified**	**Same as Report (SAR)**	**16**	

Previously, the behavior of such structure was analyzed by examining a finite horizontal "slice" of the centerline of the backwall and sidewall and treating the "slice" as a beam-column connection (Krauthammer and Marx, 1994). The results of that analysis showed that the deflections of the backwall and sidewall were excessively large, and various options for controlling the connection response were studied. Because the analysis represented essentially a two dimensional structural system, the membrane effects of the roof, backwall and sidewall were not taken into account. Further research was required to also consider these effects.

Here, however, the structure under consideration, as shown in Figure 1, was considered as a three dimensional configuration. Taking advantage of the planes of symmetry, the finite element model was generated by taking sections along the centerlines of the backwall, sidewall, and roof. In other words, this model represents one eighth of the total structure. This three dimensional model could best describe the interdependency between the individual structural component responses (i.e., the backwall, sidewall, and roof) and the system response under the effects of the 'design load'.

In order to better understand and document the contributions of each reinforcement component, ten different case models were considered using incrementally varying details of the reinforcement, as will be further discussed. In addition to the varying reinforcement details, the effect of gravity was included in some of the models to identify its effect on the behavior, and to more accurately represent the actual structure. An in-depth analysis of stresses and deformations was performed at critical locations (e.g., centerlines of the walls and roof, plastic hinge locations, etc.) to determine and define the extent of damage. Each of the cases is briefly described next, followed by a detailed discussion.

PARAMETRIC STUDY DESCRIPTION

Table 1 contains the number of 8-node concrete, 2-node steel beam, and 4- node steel thin shells used in each case, as described next and as illustrated in Figures 2a and 2b.

CASE 1: This model consists of plain concrete elements only. The elements used to model the concrete is an 8-node solid element. The sidewall and backwall had three elements through the thickness while the roof had four elements through its thickness. All subsequent models had the same concrete mesh configuration as in this model.

CASE 2: This model included the flexural and tension reinforcement as thin layers of steel represented by thin shell elements. This configuration was essentially a "smearing" of the steel reinforcing bars into thin steel layers. The volume of flexural and tension reinforcement was lumped into two layers. The two steel layers were then connected to the inner and outer surfaces of the backwall, sidewall, and roof. The volume of reinforcement used to calculate the equivalent thicknesses of the steel layers was taken from the structural details provided by NAVFAC.

Figure 1 Structure Under Consideration

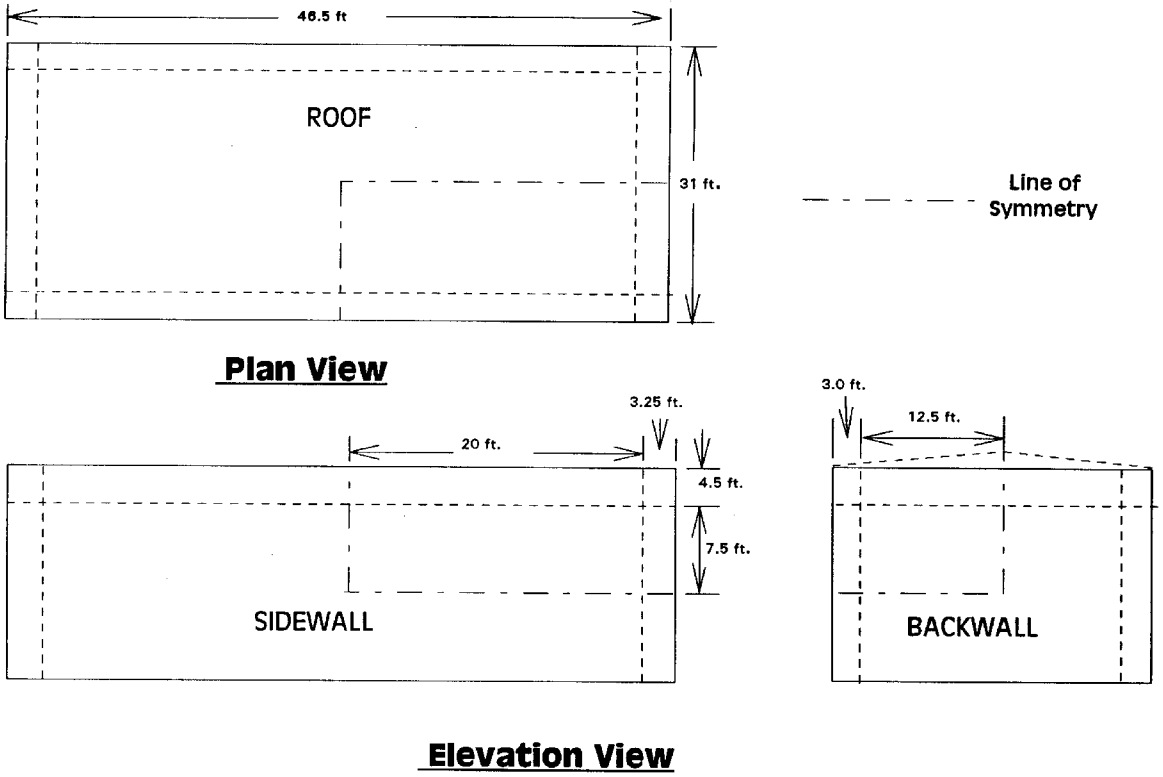

Figure 1 Structure Under Consideration

Figure 2a Reinforcement Details

Figure 2a Reinforcement Details

Figure 2b Combined Steel and Concrete Elements

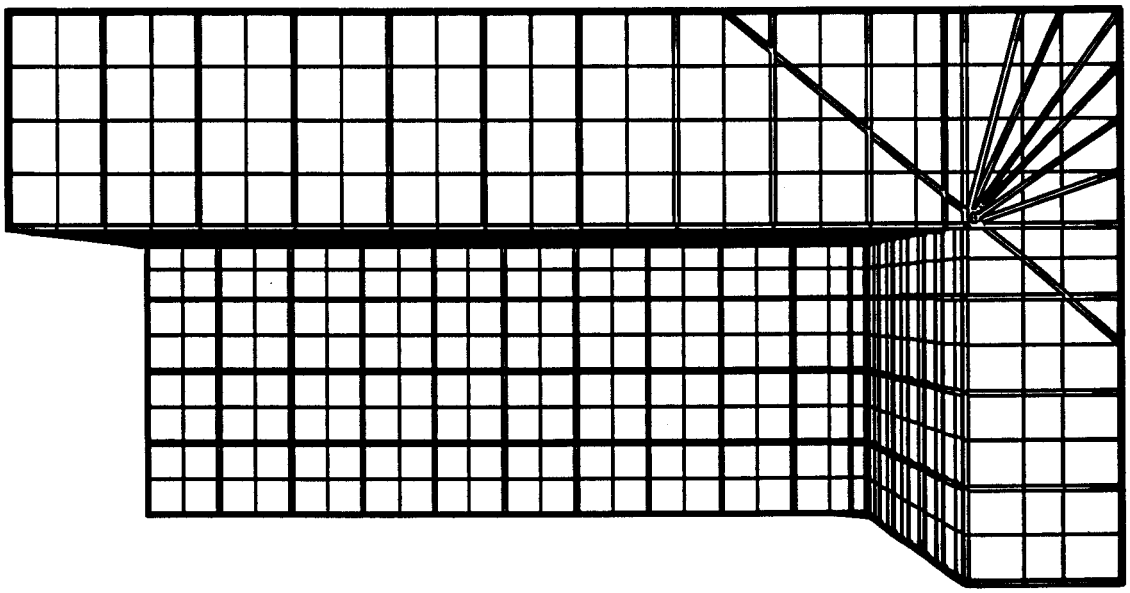

Figure 2b Combined Steel and Concrete Elements

Table 1 Element Types and Numbers for Analyses

CASE No.	Concrete Elements (8 node solids)	Steel Beam Elements (2 node beam)	Steel Shell Elements (4 node thin shells)
1	2424	0	0
2	2424	0	1728
3	2424	1456	0
4	2424	1511	0
5	2424	1511	0
6	2424	2035	0
7	2424	2163	0
8	2424	1511	0
9	2424	1519	0
10	2424	2163	0

Table 1 Element Types and Numbers for Analyses

The material model used to define the mechanical properties of the steel reinforcement was an elasto-plastic model with a linear strain hardening parameter.

CASE 3: Similarly to Case 2, this case included only longitudinal reinforcement, but it was represented as discrete steel bars modeled as tubular beam elements. Again the reinforcement was arranged on the inner and outer surfaces of the backwall, sidewall, and roof. The total area of steel was the same as per the details provided by NAVFAC, but the spacing of the horizontal and vertical reinforcement was increased to 24 inches. This simplified the details of the steel cage yet still maintained the specified reinforcement ratios.

CASE 4: The same as Case 3 but included the diagonal reinforcement at the connections. As for the flexural and tension reinforcement, the spacing of the diagonal reinforcement was 24 inches, yet it still maintained the same cross sectional area of steel as specified by NAVFAC.

CASE 5: Exactly the same as case 4, but the acceleration due to gravity was applied to the entire structure prior to the initiation of the blast load. The gravitational acceleration mainly

was applied to the structure to determine its effect on the behavior.
CASE 6: The same as Case 5 but included the shear reinforcement. Similar to the lumping of the flexural, tension, and diagonal reinforcing bars, the shear stirrup configuration was altered and lumped into a 24 inch by 24 inch mesh. The 24 inch by 24 inch configuration resulted in the steel stirrups being connected to each flexural/tension reinforcement intersection. Again the total area of shear reinforcement remained unchanged.

CASE 7: It was the closest representation of the structure under consideration, as shown in Figure 2. This model was the same as Case 6 except that the radial reinforcing stirrups were added to the corner connections. The angular spacing and the center to center spacing of the stirrups was different than specified by NAVFAC, but the total area of stirrups remained unchanged. This model was studied in the greatest detail. At the critical sections along the planes of symmetry, the maximum and minimum principal stresses of the concrete elements were analyzed to determine the extent of damage. The resultant forces of the flexural/tension and diagonal reinforcing bars were also studied to determine if yielding and/or failure of the bars had occurred at the critical sections.

CASE 8: The same as Case 7 except that all the diagonal bars were moved a distance of 12 inches inward (i.e., towards the center of structure). The cross sectional area of reinforcement was not changed. The objective was to determine the effect of an increased moment arm of the diagonals.

CASE 9: The same as Case 7 except that there was a variation in the length of the diagonal bars. At each connection, the diagonal bars were shortened so that they did not extend from outside face to outside face of the connection. This was done to evaluate the effects of the bar length and anchorage on both the global and local structural response.

CASE 10: Identical to Case 7 except that the blast loading function was changed. The blast loading was altered to determine the response of the test cell subjected only to the shock overpressure of the blast loading (see Figure 3). The gas overpressure was removed from the loading function. The change in the blast loading was to determine if the response of the structure subjected to the blast load is impulsive or dynamic in nature.

MATERIAL PROPERTIES AND LOADING

As in the previous study (Krauthammer and Marx, 1994), the material models for the structures under consideration were obtained by using the design material properties, and adjusting the soil and crushable foam material model in DYNA3D to simulate the these properties. This material model was tested by simulating experimental data obtained by other investigators, as described by Krauthammer and Marx (1994). The following material properties were used for all computations: Concrete: f'_c (uniaxial compressive strength) of 4000 psi, and ν (poisson's ratio) of 0.16. Steel: E (elastic modulus) of $29X10^6$ psi, ν (poisson's ratio) of 0.33, f_y (yield strength) of $6X10^4$ psi, and E_t (tangent modulus) of $5.1X10^5$ psi.

The design load simulated a 300 lbs TNT contained explosion with prescribed venting. The

loading function was bilinear, consisting of a shock overpressure and a gas overpressure, as shown in Figure 3. For each case, the roof and sidewall were subjected to a blast load with a peak pressure of 1115 psi, while the backwall loading had a peak pressure of 2470 psi.

Figure 3 Load Functions

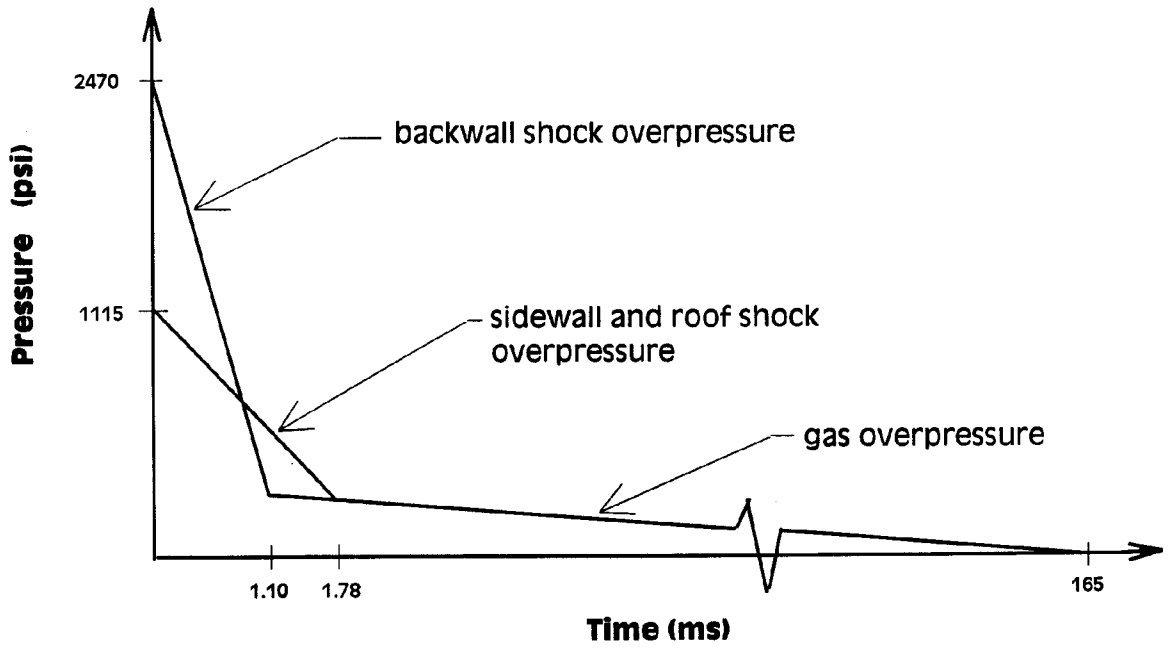

Figure 3 Load Functions

RESULTS AND DISCUSSION

The main objective of generating and analyzing the ten different case models was to systematically determine the overall effects of each type of reinforcement as it was added to the structure. Table 2 contains the maximum displacements and its corresponding time for each case. Analyses were run to a maximum of 180 milliseconds except for Case 1 which was run to a maximum time of 300 milliseconds. Even after 300 milliseconds, Case 1 did not have the required resistance to reach a stable configuration for neither the walls nor roof. For comparison to the subsequent cases, a displacement at t=180 ms for Case 1 is shown in Table 2.

Table 2 Maximum Displacements

Case No.	Backwall Δ_{max}(in)	t_{max} (ms)[1]	Sidewall Δ_{max}(in)	t_{max} (ms)[1]	Roof Δ_{max}(in)	t_{max} (ms)[1]
1	127.0*	180	182.0*	180	167.0*	180
2	19.52	57	24.71	67	43.27	105
3	24.50	68	28.35	75	57.24	135
4	11.89	50	14.93	68	33.62	110
5	13.70	45	15.70	55	33.87	105
6	9.68	40	13.00	55	30.06	100
7	9.69	40	12.02	52	28.63	100
8	6.87	30	8.37	40	24.97	100
9	15.76	50	18.06	60	34.64	110
10	1.58	18	1.54	20	2.89	47

* Does not represent Δ_{max}, a displacement and time @ t=180 milliseconds is shown for comparison to the subsequent cases.

[1] All times in the tables and figures refer to the time after the loading function has been applied.

Table 2 Maximum Displacements

Cases 2 and 3 showed the significant strengthening of the structure with just the flexural and tension reinforcement added to the plain concrete model. There was a definite plateau of displacement for cases 2 and 3, but still the displacements were very large and failure of the structural corner connections was probable.

To further strengthen the corner connections, the diagonal reinforcing bars were added to the structure for Case 4. The addition of the diagonal reinforcing bars provided a reduction in displacement of approximately (see Table 2) 41%, 47%, and 50% for the roof, sidewall, and backwall, respectively.

For the first four cases, gravitational body forces were not applied to the structure for simplicity and because of the additional computation time required gravity initialization (the load function was applied after 200 milliseconds of gravity initialization). But since displacements were still considerably large, the acceleration due to gravity was applied to the

model for Case 5 to see if the gravitational body forces had any significant effect on the overall structure. As was expected, the displacements of the roof decreased slightly due to the gravitational body forces acting directly opposite to the blast pressure, and there was a slight increase in the backwall and sidewall displacements. This increase in displacement in both walls was due to the decreased force produced in the diagonal reinforcement bars resulting from the decrease in displacement from the roof.

Case 6 included further enhancement by considering the shear reinforcement. The addition of the shear reinforcement resulted in a decrease of the maximum displacements of 29.34 %, 17.20 %, and 11.25 % for the backwall, sidewall, and roof, respectively, as shown in Table 2.

Case 7 was the model which most closely represented the actual structure. Radial stirrups at the corner joints were added to the model of Case 6. Although there was little deformation at the corner joints in Case 6, the radial stirrups were added to the structure for completeness. The addition of the radial stirrups had a relatively minor effect on the displacements, as shown in Table 2. There was essentially no change of the maximum displacement for the backwall, but there were decreases of the maximum displacements for the sidewall and roof of 7.54% and 4.66%, respectively.

Because of the significant strengthening of the connections due to the diagonal reinforcing bars, the placement of the diagonal bars were changed to assess the effects of the diagonals in a different location. For Case 8, the diagonal reinforcing bars were moved a distance of 12 inches towards the center of the structure, thus providing a larger moment arm to resist the opening of the connections. The decrease, as compared to Case 7, in the backwall and sidewall displacements of 29% and 30%, respectively, as shown in Table 2, demonstrated that the moment arm of the diagonals had a significant effect on the overall structural response. But in the case of the roof, there was only a decrease in deflection of 12.78%. The disparity between the relative responses of both walls compared to the roof is most probably due to the following two reasons: First, the relative distance that the diagonal was extended compared to the total length of the centerline plane that it was extended on. Second, the roof area is significantly larger and the blast effect is more dominant. Thus, improved detailing contributes less to remedy the roof's response. This is confirmed also by the observation that the gradual improvements in the roof deflections is less significant than that for the walls.

Case 9 included the same configuration as Case 7 except that the diagonal bars for each joint were shortened to explore the need for anchorage (these bars were terminated one element before reaching the outer main bars). Compared to Case 7, the maximum displacements of Case 9 were substantially larger, as shown in Table 2. The maximum displacements increased by 62.6%, 50.2%, and 21% for the backwall, sidewall, and roof, respectively. It is noted the behavior of this case is between Cases 3 and 4, i.e., it is better than in Case 3 (only longitudinal reinforcement), but not as good as Case 4 (full length, well anchored diagonal bars).

The loading function shown in Figure 3 exhibits a bilinear relationship consisting of the initial shock overpressure and the gas overpressure. Case 10 was carried out to determine the

response of the structure subjected only to the initial shock overpressure. The maximum displacements of Case 10 were quite small, as shown in Table 2. This indicated that the structure was stiff enough to withstand the initial shock overpressure without significant effects, and the large displacements associated with the blast loading is mainly a result of the addition of the gas overpressure.

The results of Case 7, which is the closest to the actual structural configuration, are examined in greater detail. Along the centerline planes of symmetry, where the greatest displacements and stresses occur, the maximum and minimum principal stresses at each concrete element along the critical planes (Backwall/Sidewall, Backwall/Roof, and Sidewall/Roof) were analyzed. The resultant forces of the reinforcing bars were also examined to determine if there was yielding and/or failure of the reinforcement.

The addition of the diagonals resulted in a significant strengthening of the structure yet further examination of the deformed structure revealed the formation of plastic hinges near the ends of the diagonal bars. The plastic hinges were characterized by very large local rotations. These rotations are important because of the associated high stresses. Table 3 contains a summary of the local and global joint rotations for each connection, as defined in Figure 4.

The local and global rotations are a good indication of the extent of damage in a connection. The connections with the largest rotations had the largest extent of damage. The locations of the plastic hinge was characterized by a large discontinuity of rotation near the ends of the diagonal bars, as shown in Figure 4. The flexural/tension reinforcing bars and the diagonal bars were examined to determine their conditions, as summarized in Table 4 in terms of their maximum stresses for each connection. In Case 6, the shear stirrup reinforcement was added to the test cell model to determine the effect of the stirrups. Each stirrup at the critical section was checked to determine if there was any yielding in the shear reinforcement. None of the stirrups at the critical sections had reached their yield stress, the shear reinforcement helped to strengthen the area near the diagonals.

Table 3 Global and Local Rotations

Connection	Side	θ_1	θ_2
Backwall/Roof	Roof	18.03°	6.80°
	Backwall	14.37°	6.15°
Sidewall/Roof	Sidewall	18.77°	7.61°
	Roof	22.17°	10.81°
Sidewall/Backwall	Sidewall	13.70°	2.87°
	Backwall	14.77°	3.70°

θ_1=Local Joint Rotation
θ_2=Global Joint Rotation

Table 3 Global and Local Rotations

Figure 4 Structural Rotations

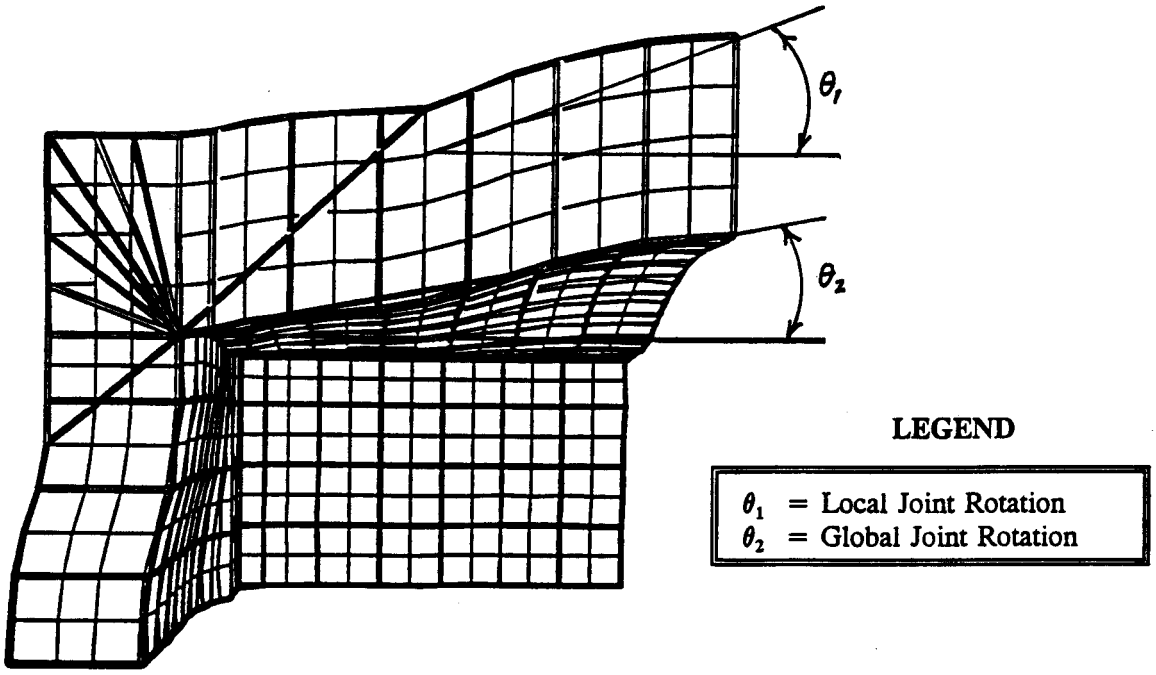

Figure 4 Structural Rotations

Table 4 Maximum Steel Stresses

CONNECTION	BAR TYPE	STRESS (ksi)
Backwall/Roof	Diagonal	67.313
	Flexural/ Tension	100.809
Sidewall/Roof	Diagonal	88.225
	Flexural/ Tension	101.998
Sidewall/Backwall	Diagonal	55.271
	Flexural/ Tension	101.830

Note: $\sigma_y = 60$ ksi

Table 4 Maximum Steel Stresses

CONCLUSIONS

The three dimensional analysis of the blast containment structure under consideration is a realistic method of modelling and simulation. By performing the three dimensional analyses, the membrane stiffening effects of the walls and roof are taken into account whereas in the two dimensional analysis, the membrane effects are neglected. The results of this study capture the incremental strengthening of the overall structure as each reinforcing component is added to the structure. The addition of the flexural/tension reinforcement provided substantial strength enhancement compared to the plain concrete model, but the displacements were still very large.

The diagonal bars had the most significant strengthening effect on the structure, and resulted in very large reductions of displacements. At the corner connections, the opening of the corner joints was very small thereby minimizing the stresses within the joints. The placement of the diagonal bars is also very important. The extension of the moment arm of the diagonal bars resulted in an even further strengthening of the structure. But in Case 9, where the diagonals were shortened so that they did not extend from outside face to outside face, the structure exhibited larger deformations. This observation highlights the requirement for diagonal bars to extend from outside face to outside face of the connection and be well anchored in order to obtain their full contribution.

Examination of the stresses in the connections of Case 7 revealed that yielding of the longitudinal

and diagonal reinforcement would result from the blast load. The yielding of the reinforcement is associated with the formation of plastic hinges near the endpoints of the diagonal bars. These hinges are characterized by large localized rotations, and this adverse condition is complicated further by the presence of both tension (associated with the expanding structure) and shear (due to the geometric variation of the cross-section). In addition to the damage to the steel, there were significant concrete tension failures at these locations, and the stress patterns served as good indicators of the corresponding damage that could occur. It should be noted that TM 5-1300 does not explicitly address the issue of plastic hinges, and it does not contain guidance on how to design such regions.

It was noted that the values of θ_1 (i.e., the local rotations, as defined in Figure 4) exceed the maximum support rotations of 12°, as specified in Table 4-2 of TM 5-1300. The values of θ_2 (i.e., the global rotations, as defined in Figure 4) for the sidewall/backwall connection exceeds 2°, while for the backwall/roof and sidewall/roof it exceeds 5°. However, θ_2 values are less than 12°. This highlights the need to address localized rotations in TM 5-1300, and to differentiate between local or global rotations in the design process.

The addition of the shear reinforcement provided substantial strengthening near the plastic hinge locations, where the largest shear stresses occurred, and the shear deformations in the concrete elements were reduced considerably. Although, the radial stirrups had little effect on the overall structural response, they contributed to enhancing the integrity of the connections.

When the loading function was altered to include only the shock overpressure, the structure exhibited very small deformations. Therefore, if the gas overpressure of the loading can be reduced by means of improved venting, the corresponding structural deformations could be decreased significantly. This could have a significant positive influence on the requirements for the wall thicknesses and reinforcement details.

The analyses of the present structure resulted in the determination of its alterable behavior due to the varying reinforcement details. The model used in all the cases was a derivative of Case 1 consisting of 2424 3D solid concrete elements. In all the subsequent cases, the reinforcement details were gradually altered to assess their incremental contributions to the behavior, but they conform to the same nodal mesh. In current analyses, the resolution of the nodal mesh has been increased significantly (by a factor of about 40) so that the reinforcement details of the finite element model conform accurately to the specific aspects of the structure. This will allow a more precise analysis of the behavior, motions and stresses, and better damage predictions. Additional information on these issues is anticipated from planned experiments that were designed to capture also data related to these findings.

REFERENCES

Department of the Army, "Structures to Resist the Effects of Accidental Explosions", TM 5-1300, November 1990.

Krauthammer, T., and Marx, E., "Combined Numerical Experimental Development of Innovative Structural Concrete Connections", in: Building the Future, edited by F.K. Garas, G.S.T. Armer, and J.L. Clarke, E & FN SPON (Chapman & Hall), London, 1994.

NCEL, "Basis of Design for NAVFAC Type I Missile Test Cell", Technical Note N-1752R, Revision 1, April 1990.

Whirley, R.G., and Engelmann, B.E., "DYNA3D User Manual", UCRL-MA-107254 Rev. 1, Lawrence Livermore National Laboratory, Nov. 1993.